Journal of Archaeological Science: Reports 70 (2026) 105557

Contents lists available at ScienceDirect

Journal of Archaeological Science: Reports

journal homepage: www.elsevier.com/locate/jasrep

"From blue to red: first evidence of heat treatment in the production of Minoan serpentinite vases through non-invasive study and experimental petrology"

Killian Regnier [a,b,*], Antoine Triantafyllou [b], Jean-Philippe Perrillat [b], Charlotte Langohr [a], Gilles Montagnac [c], Clémentine Fellah [c], Jérôme Bascou [d], Anne-Christine Da Silva [e]

[a] F.R.S.-FNRS, Aegean Interdisciplinary Studies (AEGIS), Institut des Civilisations, Arts et Lettres (INCAL), Université catholique de Louvain, Collège Erasme, Place Blaise Pascal 1, 1348 Louvain-la-Neuve, Belgium
[b] Université Claude Bernard Lyon1, LGL-TPE, UMR 5276, ENS de Lyon, UJM Saint-Etienne, CNRS, Villeurbanne 69100, France
[c] ENS de Lyon, LGL-TPE, UMR 5276, Université Claude Bernard Lyon1, UJM Saint-Etienne, CNRS, Villeurbanne 69100, France
[d] Université Jean Monnet (UJM), LGL-TPE, UMR 5276, Université Claude Bernard Lyon1, ENS de Lyon, CNRS, Saint Etienne 42000, France
[e] SediCClim Laboratory, Département de Géologie, Université de Liège, B20, Allée du Six Août, 12, Quartier Agora, 4000 Liège, Belgium

ARTICLE INFO

Keywords:
Serpentinites
Protopalatial Crete
Stone heat treatment
X-Ray fluorescence
Magnetic susceptibility

ABSTRACT

The intentional heat treatment of stone to alter its appearance remains a largely understudied practice in archaeology, and its identification in the archaeological record is often challenging. By combining portable and non-invasive X-ray fluorescence (pXRF) and magnetic susceptibility (pMS) analyses with controlled heating experiments on local serpentinite used in Minoan (Bronze Age Crete) contexts, this study presents the first documented evidence of intentional heating in the production of stone vases. It also proposes a replicable analytical framework broadly applicable, yet particularly suited to ultramafic lithologies. It focuses on a unique assemblage from the late Protopalatial period at *Quartier Mu*, Malia (Crete, 1800–1700 BCE), where twenty-five serpentinite vases exhibit a distinct red coloration.

Macro-petrographic observations and pXRF analyses confirm that the red vases consist of serpentinite and show no trace of added pigments. pMS values are significantly lower in the red serpentinite vases than in the blueish (unheated) ones, which is consistent with the effect of heating samples of Cretan serpentinite in our experimental results. In our high-temperature heating experiments, the red coloration is driven by the natural transformation of magnetite into low-magnetic iron oxides at temperatures above 700 °C under oxidising conditions. The application of this thermal threshold, combined with contextual evidence showing no signs of large-scale burning, allows us to reject the hypothesis of accidental firing.

These findings provide new insights into Minoan stone-vase production, identifying heat treatment as a deliberate technological choice at *Quartier Mu*. More broadly, the methodology illustrates how experimental petrology and non-invasive techniques can together highlight ancient heat-related practices while preserving the artifacts.

1. Introduction

Stone vases represent a significant aspect of Minoan Bronze Age Cretan craftsmanship. The choice of various materials, including serpentinite, chlorite-rich rocks, and limestone, reflects both resource availability and technological expertise since their production involves advanced carving and polishing techniques highlighting the artisans' skills (Morero, 2016). Serpentinite, which is specifically investigated in the present article, is one of the metamorphic rocks widely used in human history as building materials and ornamental stones for its appealing appearance and color (Punturo et al., 2018). It is a rock mostly composed of serpentine minerals (lizardite, chrysotile, and antigorite), formed through the alteration and/or metamorphism of mafic to ultramafic rocks, mainly peridotites (Deschamps et al., 2013).

More than a thousand Minoan stone vases have been found in various contexts (Bevan, 2007; Warren, 1969), illustrating their diversity and

* Corresponding author at: Collège Erasme, Place Blaise Pascal 1, bte L3.03.01, 1348 Louvain-la-Neuve, Belgium.
E-mail address: Killian.regnier@uclouvain.be (K. Regnier).

https://doi.org/10.1016/j.jasrep.2025.105557
Received 8 October 2025; Received in revised form 15 December 2025; Accepted 15 December 2025
Available online 18 January 2026

length of use (2650–1450 BCE). Their presence in high-status assemblages suggests that they played a role in elite consumption and ceremonial practices, while their widespread distribution across Crete in funerary and domestic contexts also indicates active trade and exchange networks among more common people (*e.g.*, Detournay, 1980; Relaki and Tsoraki, 2015; Flouda et al., 2020).

This study examines the exceptionally well-preserved archaeological context of *Quartier Mu* at Malia (1800–1700 BCE), a key site for understanding the Protopalatial period in Minoan Crete (Fig. 1). As a contemporary complex of the first Minoan palaces during the Middle Bronze Age, *Quartier Mu* offers critical insights into the sociopolitical developments of this timespan marked by the transition from the small Prepalatial communities to the so-called "Neopalatial states" (Driessen, 2024, pp. 14–15).

1.1. Quartier Mu and its stone vases

Quartier Mu is an important complex known for its exceptional preservation thanks to it being sealed by a thick layer of clay resulting from the melting of its mudbrick architecture during its violent destruction (Poursat and Knappett, 2005, p. 1). The materials found include a variety of items such as domestic ceramics, glyptic production, stone tools and vases, as well as precious objects like jewellery, metal vases, elaborately decorated pottery and even gold-decorated weapons. The quarter includes ten buildings, among which four are commonly identified as workshops for the production of seals, ceramic vases and metal objects (*atelier des Sceaux*, *atelier de Potier*, *atelier de Fondeur* and *atelier Sud*), and two as ceremonial and administrative buildings (buildings A and B), the remaining ones being interpreted as annexes or storage facilities (buildings C to F) (Fig. 2) (Schmid and Treuil, 2017, pp. 9–10).

The production and use of stone vases in *Quartier Mu* reflect both continuity and innovation within the broader Minoan tradition. While the previous Prepalatial period (2650–1900 BCE) sees the use of various stone types and the genesis of a variety of vessel forms, the Protopalatial era is marked by an increase in standardised shapes and the widespread use of serpentinite, likely linked to specialised workshops and evolving craft traditions (Morero, 2016, p. 28). The assemblage from *Quartier Mu*, consisting of more than 350 stone-vessel fragments, illustrates this development, with serpentinite being the predominant material, alongside smaller quantities of limestone, breccia, and marble (Detournay, 1980, p. 66).

Among this assemblage, twenty-five vases stand out owing to their distinctive red coloration (Figs. 3 and 4). Unpublished geochemical whole-rock analyses show that they are ultramafic ($SiO_2 < 45$ wt%) and led to the hypothesis that they are made of heated serpentinite (Detournay, 1980, p. 65)[1]. Although some researchers have proposed the existence of naturally red serpentinite in Crete (Krzyszkowska, 2018), this study argues that the red colour of the *Quartier Mu* vases is unlikely to come from such raw materials (see Discussion 4.1). This raises questions about the conditions required to achieve this coloration and whether it was a deliberate modification or an unintended result of the destructive fire. At first glance, it has been suggested that the red coloration of these vases resulted from intentional heating, as there are examples of visibly burnt serpentinite vases that have retained their original blue colour (Detournay, 1980, p. 67). However, the localised presence of heavily vitrified ceramics can suggest that only specific areas of the building were exposed to exceptionally high temperatures during its destruction, allowing only some serpentinite vase fragments to be sufficiently fired to turn red (Bevan, 2007, p. 254, n. 10). It has also been suggested that the red coloration of the vases was intentional since it could not be the result of a simple heating of "serpentine", as "serpentine" contains a low fraction of iron oxide (Morero, 2014a, p. 83; 2014b, p. 351). E. Morero, however, does not exclude the possibility that a specific type of "serpentine", richer in iron oxides, was used (Morero, 2014b, p. 352)[2], as these oxides are well known to produce different hues of red upon heating (Schwertmann, 1993).

This study aims, on one hand, to determine whether the red coloration observed on serpentinite vases from *Quartier Mu* resulted from intentional heating or accidental exposure to fire and, on the other hand, to constrain the thermal conditions. By integrating non-invasive analyses of the archaeological materials with experimental heating petrology on serpentinite rock samples, we seek to replicate the transformations observed in the archaeological materials under controlled conditions with similar starting materials. This approach allows us to assess the feasibility of intentional heat treatment but also to define different temperature thresholds and material properties influencing colour transformation. The intentional versus accidental heating is further considered by recontextualising the red vases within their whole assemblages and by evaluating their spatial distribution within *Quartier Mu.* This recontextualisation makes it possible to explore whether this heat treatment was employed as a multicraft strategy potentially linked to the technological exchanges and innovations made by artisans in the quarter.

2. Archaeological materials study

2.1. Description of the assemblage

Serpentinite vases from *Quartier Mu* account for 85 out of the 166 non-red examples studied by B. Detournay (1980). The twenty five red vases from *Quartier Mu* include eleven bowls, five lids, three handled cups, two teapots, one libation table, one bird's nest vase, one miniature vase, and one spout of unidentified typological affiliation (Detournay, 1980). All these forms are common within the Protopalatial period (Warren, 1969), and they all correspond to the non-red serpentinite vases recovered in the *Quartier*, except for the teapots, the libation table, and the miniature vase which have been found only in the red version. In terms of spatial distribution, the reddened vases exhibit a distinct clustering, in contrast to the relatively uniform dispersion of non-red serpentinite vase fragments across the quarter (Fig. 2). Seventeen of the twenty-five red vases come from Sector V of Building B and seven from Building A (four of which were in Room I 5)

During a first macroscopic study campaign on the stone vases from *Quartier Mu*, we were able to macroscopically classify 100 vases, among which 47 serpentinite vases, 11 red vases, 28 vases made in other stones and 14 unclassified. Among the serpentinite items, 22 were of a similar lithotype. This facies presents a dark blueish matrix with millimetric to centimetric lighter patches, possibly serpentinised pyroxene – so-called "bastite" (Debret, 2013, p. 39). Some of the blue matrix also display dark veins typically found in serpentinised ultramafic rocks and likely made of magnetite (Hodel et al., 2017) (Fig. 3). There is a strong similarity between these facies and most of the red vases (Figs. 3 and 4). A second study campaign allowed us to analyse 16 dark-blueish serpentinite vases and 9 of the red vases. The selection was based on the best-preserved specimens, the surfaces of which allowed for reliable macroscopic and analytical observations. Among the red vases, three specimens display a clear section, with a colour gradient from a deep red outer rim gradually fading to a greyish core. The rim thickness varies between objects, but it is consistently pluri-millimetric and follows the carved contours of the vases (Fig. 5).

[1] Pers. com. with J.-Cl. Poursat, head of the excavations, yielded only a single geochemical result for an unidentified red vase, which corresponds to the geochemistry of an ultramafic rock.

[2] This precision is close to the truth considering that her previous remark conflates the mineral serpentine [$(Mg,Fe,Ni)_3Si_2O_5(OH)_4$] with the rock serpentinite, the latter being the material actually used for the vases and containing both serpentine and accessory minerals, notably different iron oxides.

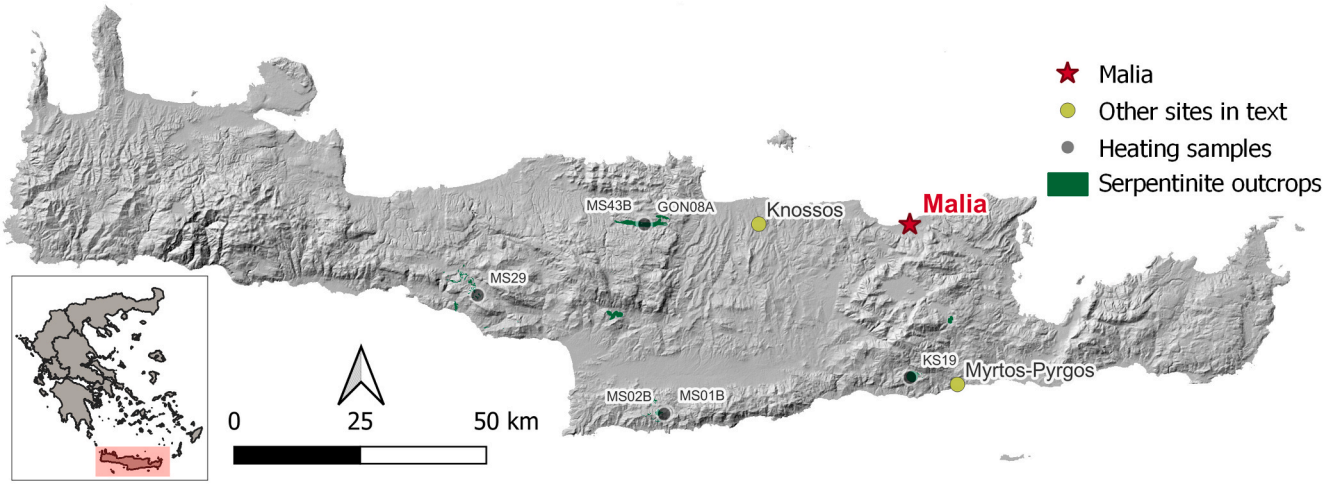

Fig. 1. Map of Crete with sites mentioned in the text, serpentinite outcrops and location of rock samples used in the heating experiments. Serpentinite outcrops are based on (Becker, 1975, 1976; Martha et al., 2019, 2017; Tortorici et al., 2012).

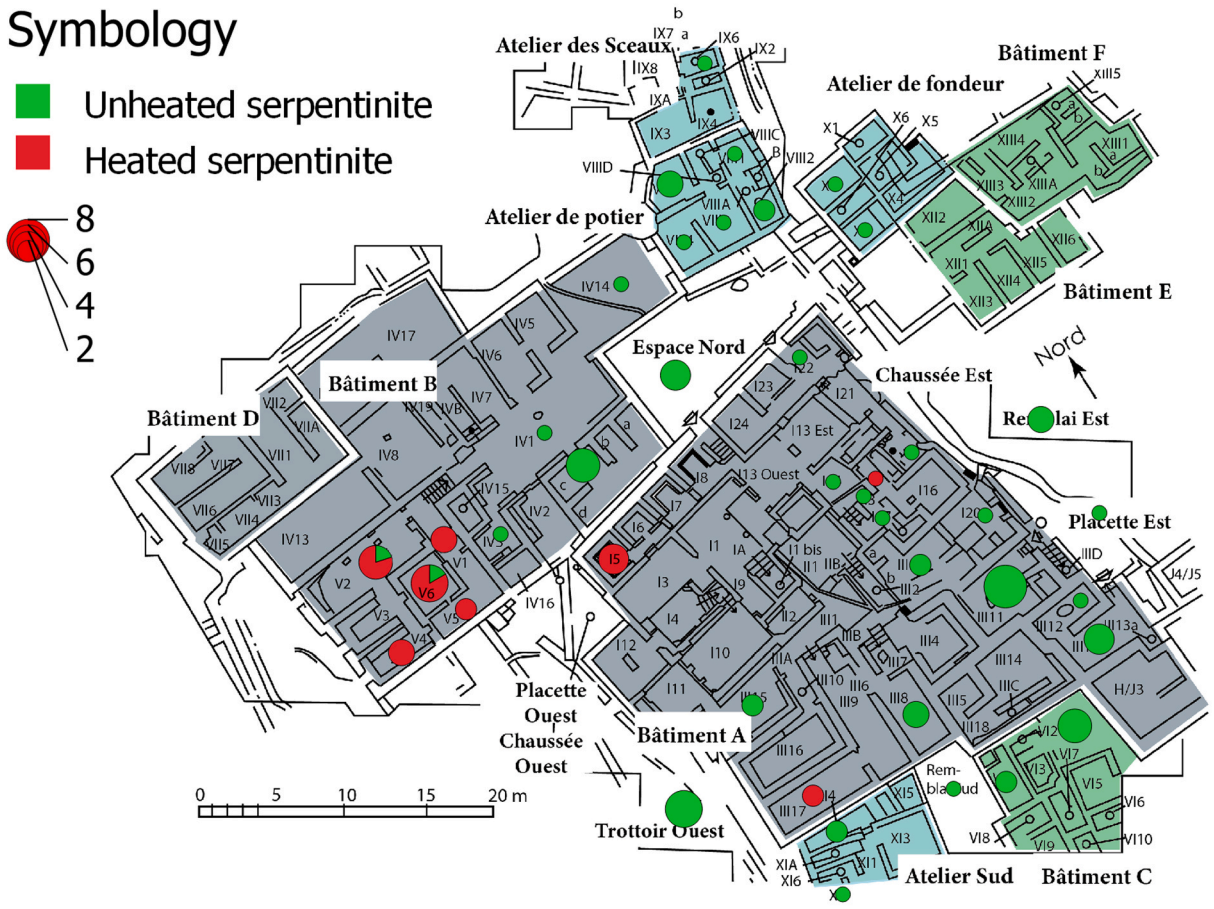

Fig. 2. Plan of Quartier Mu with repartition of serpentinite vases with data from Poursat, 1996 and Dubois, 2017. (Background plan courtesy of B. Rueff; edited by K. Regnier).

2.2. Methods

We applied fully portable and non-invasive methods to characterise the geochemistry and magnetic susceptibility of the archaeological materials. Geochemical analyses were performed with a SciAps X-505 energy dispersive portable X-Ray fluorescence (pXRF) device. This method enables the *in situ* determination of the elemental composition of the samples, providing valuable insight into their overall geochemical signature. Notably, pXRF allows a clear discrimination between serpentinitic and amphibole asbestos phases (Bloise and Miriello, 2018). Following the calibration scheme proposed by Da Silva et al. (2023) for geological samples, major element concentrations were determined with an accuracy of >95 % based on 27 magmatic standards. Further details are presented in Appendix A.1 pXRF.

Fig. 3. The first lithotype at *Quartier Mu*. All photos to scale and calibrated. Dashed circles are spots used in Fig. 9. Top row, left to right: 66 M613, 67 M792, 69 M1530; bottom row, left to right: 68 M213, 88–1029-04, 69 M1404 (© EfA, Hellenic Ministry of Culture; photos by K. R.).

Fig. 4. Examples of red vases at *Quartier Mu*. All photos calibrated. Dashed circles are spots used in Fig. 9. Top row, left to right: M67/80, 67 M569, 70 M76; bottom row, left to right: 66M162a, 67 M378, 67 M381 (© EfA, Hellenic Ministry of Culture; photos by K. R.).

Magnetic susceptibility is a rapid and cost-effective method for identifying the amount of iron oxides in a rock, as most ferrous mineral phases exhibit characteristic magnetic properties (Graham, 1953). In the case of serpentinite, magnetite naturally forms through the process of serpentinisation (Chen et al., 2021), making magnetic susceptibility particularly useful for assessing mineral transformations in these rocks.

Fig. 5. Cross-sections of three vases showing a gradual colour change from the exterior to the interior, of a continuous uniform thickness. From left to right: 67 M480, 71 M851, 67 M378 (© EfA, Hellenic Ministry of Culture; photos by K. R.).

Portable magnetic susceptibility (pMS) analyses were performed using a Bartington MS2K susceptibilimeter, under a similar approach as in (Triantafyllou et al., 2021). Further methodological details can be found in Appendix A.2 pMS analyses.

2.3. Geochemical and magnetic susceptibility results

Initial observations indicate that both the blue and red vases share geochemical features characteristic of ultramafic rocks, *i.e.* a high MgO concentration and a high MgO/SiO_2 ratio between 0.5 and 0.9, with a low Al_2O_3 content mostly restricted below 5 wt% (Fig. 6a). The CaO content ranges from 0.4 to 4.7 wt% and they are rich in Ni, consistently above 1500 ppm, which suggests that they are mantle derived (Menzel et al., 2019) (Fig. 6c-d). Both the red and blue vases exhibit similar geochemical compositions, broadly consistent with the global serpentinite reference dataset (Fig. 6a–d), although slight variations are expected given that pXRF measurements, and especially lower energy X-rays, are susceptible to surface related epi-phenomena (Forster et al., 2011; Grave et al., 2012).

pMS analyses show a relatively high overall value of magnetic susceptibility (SI units), with a significant shift between the blue vases ($25.9–86.4SI \times 10^{-3}$) and the red vases, which remain below $16.9SI \times 10^{-3}$ (Fig. 7). The high value from the blue vases likely suggests the presence of maghemite and/or magnetite as these are one of the very few minerals capable of producing such elevated readings (Borradaile and Jackson, 2004; Rochette et al., 1992). Magnetite is considered here as a more probable candidate thanks to its superior stability. The combination of a geochemical signature consistent with magnesium-rich, mantle-derived rocks and a relatively high magnetic susceptibility (Bonnemains et al., 2016) supports the macroscopic interpretation that blue vases can be attributed to serpentinite lithologies. The fact that the red vases macroscopically resemble the blue vases and share the same mafic geochemical features suggests that they derive from the same lithology, but with the magnetite transformed into low-magnetic iron oxides, possibly because of heating. This hypothesis has been tested by experimental heatings, presented in the next section.

3. Heating experiments

3.1. Starting materials and experimental conditions

We conducted controlled heating experiments using Cretan serpentinite as a starting material. These experiments aimed to simulate the thermal transformations, and document the heating conditions required to induce colour changes in the serpentinite material. It is not yet possible to assess the provenance of the serpentinite used in Malia considering the high heterogeneity of this lithotype in outcrops and the absence of recognised quarries. Experimental samples have been selected after a sampling survey from different mapped serpentinite outcrops in Crete (Fig. 1). Samples were collected from both bedrock and river boulders (n = 90), as it has been suggested that such natural cobbles and boulders were an ideal source of procurement (Becker, 1975). After a pXRF and pMS analysis of all of them, six samples were selected to capture the greatest variability in terms of facies and chemical composition, encompassing the widest range of both characteristics (samples GON08A, KS19, MS01B, MS02B, MS43B and MS29). Macroscopically, samples GON08A, MS02B, and MS43B were identified as serpentinised peridotites containing visible macrocrystalline automorphic minerals, likely partially serpentinised pyroxenes. MS01B is comparable in composition but is significantly more homogeneous, with only a few visible automorphic minerals. In contrast, MS29 and KS19 are much more heterogeneous. MS29 is characterised by numerous white veins, possibly composed of talc or asbestos (tremolite/chrysotile), and a small number of automorphic minerals that seem to be highly serpentinised. KS19, on the other hand, contains few automorphic minerals, with little to no evidence of serpentinisation.

Heating experiments were conducted using a Nabertherm RT50-250/13 tube furnace under ambient air-oxidising conditions. The temperature range for heating experiments (600–1200 °C) was selected based on previous studies on serpentine dehydration and olivine oxidation (Bloise et al., 2016, Dlugogorski & Balucan, 2014; Knafelc et al., 2019). The oxidising condition, typically associated with red coloration (Frerebeau and Pernot, 2018; Lagoeiro, 1998, p. 418), was assumed to be atmospheric conditions (*c.* QFM + 10; McCammon, 2005). Each sample was cut in half, with one half being heated and the other one serving as the unheated protolith. Heated samples were cut into a square shape, about 3 cm square and 2 cm thick. Each heating consisted of a 1-hour ramp-up to the target temperature (600–1200 °C), followed by 6 h of sustained heating at that temperature, and a subsequent 2.5-hour controlled cooling period. Afterwards, each heated sample was analysed again by pXRF and pMS with the exact same acquisition parameters as those for analysing archaeological materials.

Three geological samples, MS01B, MS02B and MS43B, were powdered and analysed using X-ray Diffraction (XRD) to compare the whole-rock mineralogical composition before and after heating. XRD is a tool for accurately identifying minerals by examining their unique diffraction patterns. Further methodological details can be found in Appendix A.3 XRD analyses.

The sample with the best colour-change results, MS43B, was investigated with scanning electron microscopy and energy-dispersive X-ray microanalysis (SEM-EDS), as well as μ-Raman spectroscopy (μ-RS), to investigate how the red hue is distributed across the mineral phases. These complementary techniques allow for the identification of *in situ* mineral transformations and potential oxidation processes responsible for the development of the red colour, offering insights into thermal alteration pathways and the role of iron-bearing phases. Further methodological details can be found in Appendix A.4. μ-RS analyses and Appendix A.5. SEM-EDS analyses.

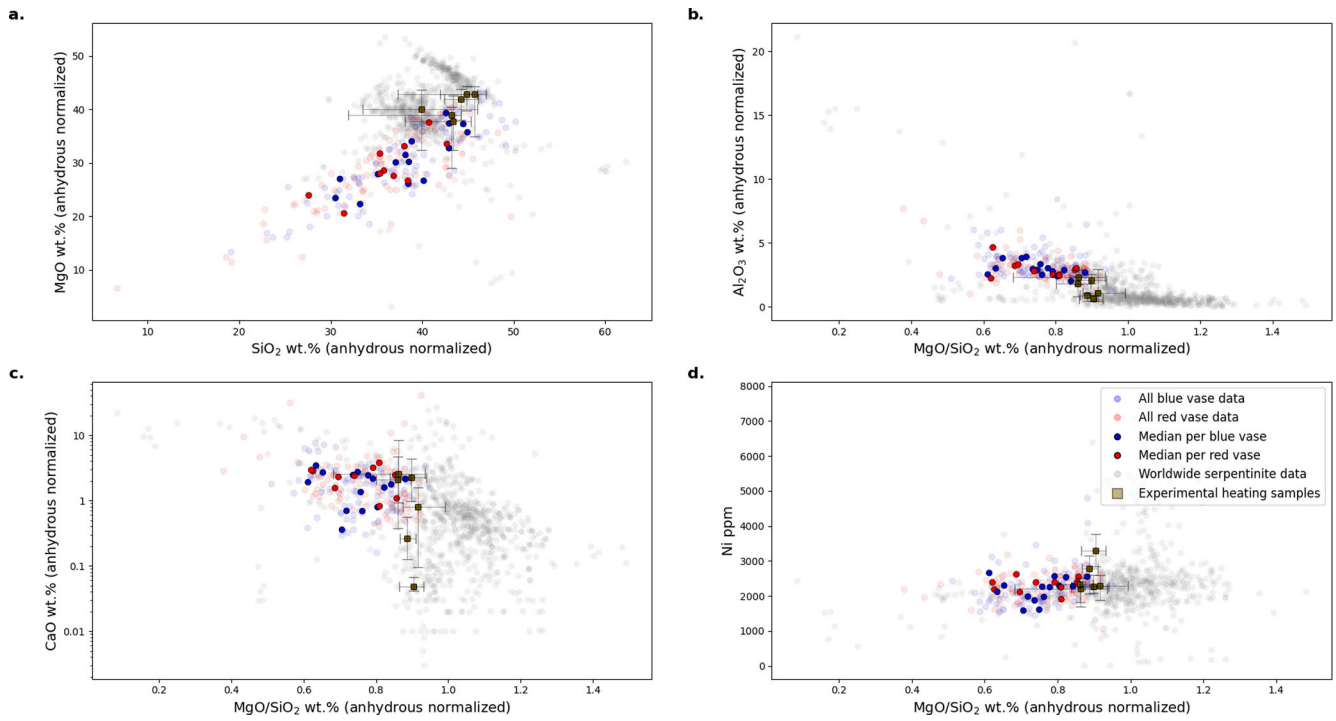

Fig. 6. pXRF analyses of stone vases from Quartier Mu a. SiO2 (wt. %), b. CaO (wt. %), c. TiO_2 (ppm), d. Ni (ppm) versus MgO (wt.%) binary diagrams. The solid points (no transparency) show the median values per vase. The coloured transparent points represent all individual data points from the analyses, while the grey transparent points are data from the subduction zone serpentinite worldwide compilation (Deschamps et al., 2013). Experimental heated samples are illustrated by their median (square) and internal heterogeneity (bars). The CaO axis is in the logarithmic scale.

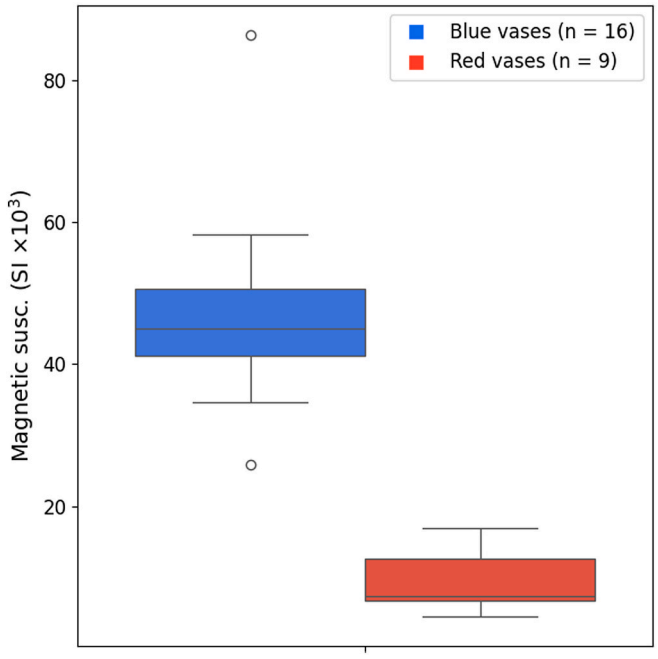

Fig. 7. Boxplot with magnetic susceptibility values for blue and red vases. For each vase, 10–20 measurements were taken, except for two vases (N = 5 and N = 9).

3.2. Results

pXRF and pMS analyses confirm that the heated samples are geochemically and magnetically comparable to the archaeological materials. Although the experimental samples display, on average, a slightly lower SiO_2/MgO ratio (1.0–1.2) compared to the archaeological objects (1.1–1.4), their CaO, Ti, and Ni contents fall well within the same compositional range (Fig. 6a–d). Additionally, all unheated samples exhibit a magnetic susceptibility above $20SI*10^{-3}$, whereas heated samples fall below this threshold, aligning very well with the values observed in the archaeological materials (Fig. 8).

Macroscopic observations. Heating experiments on sample MS43B reveal significant colour transformations depending on temperature, and indicate that a red coloration begins to develop when temperatures exceed 700 °C, culminating in a dark red–orange hue at 800–900 °C (Fig. 9). At 600 °C, only minor colour changes are visible, with dark yellow-green and brown tones, whereas at 1200 °C, the hue shifts noticeably to brown. There is also a noticeable increase in micro- to macro-fractures related to the increased temperature. The sample heated at 1200 °C became very fragile and broke during handling.

Additional tests at 800 °C on various samples reveal significant colour variations depending on the protolith (Fig. 10a and b), but all have in common that heated samples exhibit warmer hues compared to their unheated counterparts. Unheated samples predominantly exhibit dark greyish-blue and greenish-grey hues, with the heating process tending to lighten the samples, enhancing red and brown tones while also increasing saturation. Heated samples and red vases both exhibit warm hues dominated by red, brown, and orange tones, reflecting the thermal alteration effects. Red vases generally show higher brightness than the heated samples.

Microscopic and mineralogical analysis. Unheated and heated (800 °C) sample MS43B was observed using SEM-EDS and μ-RS (Fig. 11). As primary phases, the starting material shows both coarse-grained clinopyroxene and orthopyroxene (*ca.* 20 % vol.), plus fragmented olivine (*ca.* 50 % vol.). The entire rock is serpentinised (*ca.* 25 %), forming a mesh-like network transforming both olivine and orthopyroxene through their cleavages. Magnetite (*ca.* 3 % vol.) is the only oxide in the rock and forms into bands and bulk oxide. In heated samples, the mesh-like texture is perfectly preserved but the serpentine is completely transformed into forsterite, the magnesian pole of olivine, with a

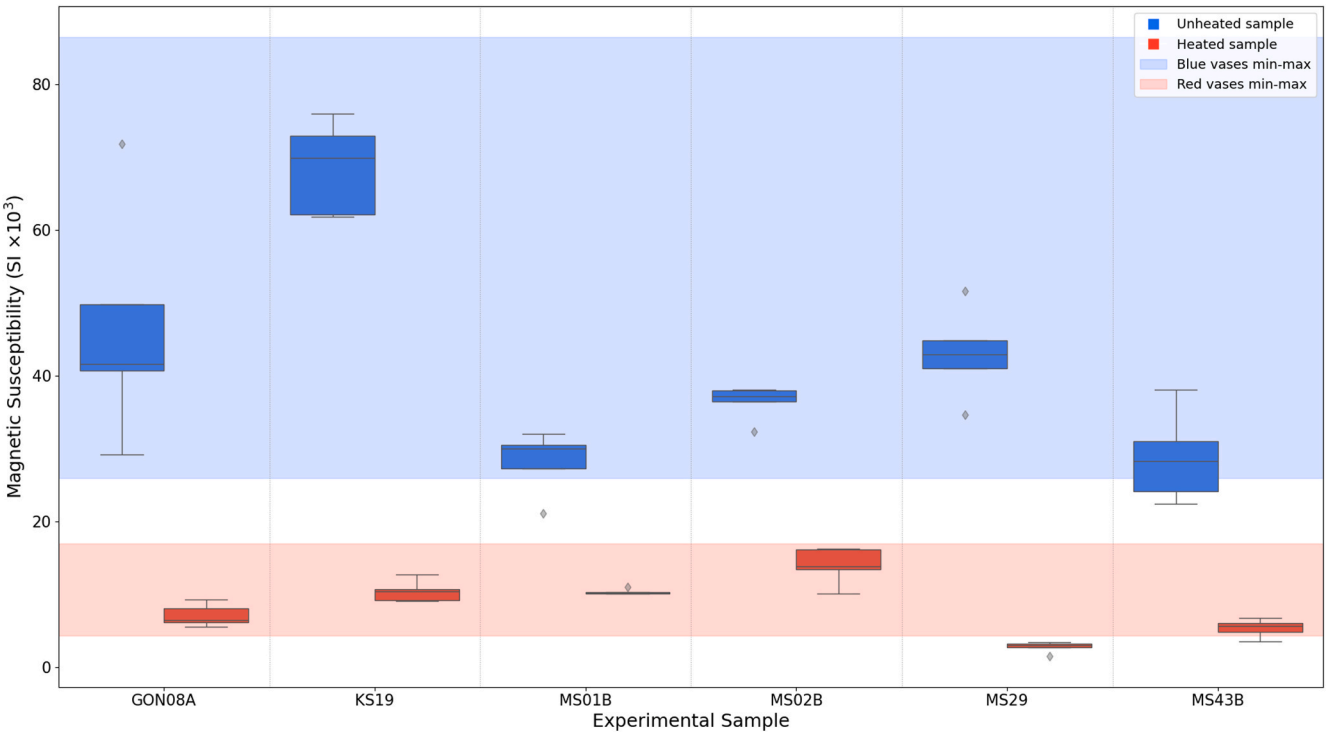

Fig. 8. Boxplot with magnetic susceptibility values before and after heating at 800 °C, with 10 analyses per boxplot. The shaded areas indicate the range observed in archaeological vases.

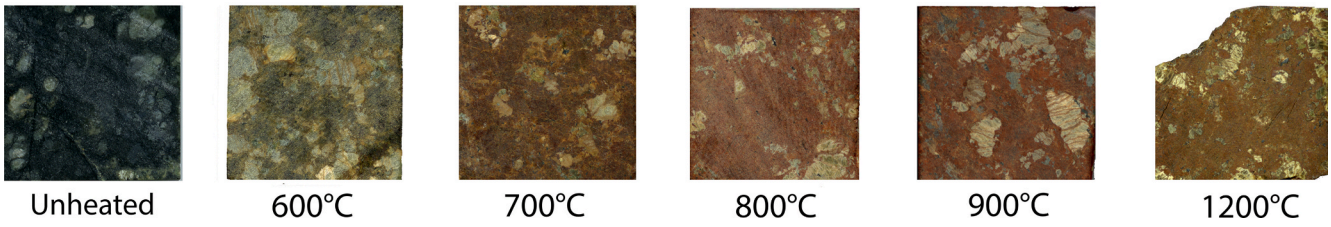

Fig. 9. High resolution scans of MS43B sample at various stages of the experimental process, subjected to different temperatures.

different composition from pristine olivine fragments (*ca.* 82.7 % Fo for pristine olivine versus *ca.* 92.1 % Fo for olivine formed after heating) (Fig. 11a and b). From previous studies, we know that this reaction can start at around 600 °C under ambient pressure and atmospheric redox conditions (Bloise et al., 2016; Dlugogorski and Balucan, 2014). As shown by Raman analyses, all magnetite grains were transformed into hematite (Fig. 11a and b). Both observations were confirmed by a whole-rock XRD analyses of three samples (Fig. 12). The distribution of newly formed hematite is like that of magnetite, just as the newly formed olivine resembles the previously described serpentinite, suggesting a pseudomorphosis for both minerals. Although not observed on back-scattered electron images, μ-RS reveals that hematite also forms within olivine (Fig. 11b). This result aligns with previous observations that naturally occurring iron in olivine $(Mg,Fe)_2[SiO_4]$ tends to nucleate along dislocations and impurities in the crystal structure to form magnetite and hematite (Knafelc et al., 2019). Heated samples are also marked by the occurrence of numerous fractures (Fig. 11b) which preferentially develop into serpentine bands but crosscut pristine pyroxene and olivine.

4. Discussion

4.1. Natural vs heated serpentinite

Since this study assumes that the red vases acquired their colour through exposure to heat rather than being made from naturally red serpentinite, the basis for this assumption must be made explicit. The main evidence comes from the cut profiles of three specimens (71 M851, 67 M378 and 67 M480; see Fig. 5), which all show a clear exterior-to-interior colour gradient, with a dense red outer layer gradually fading to light grey at the core. This pattern is absent in blue vases and therefore cannot be the result of surface weathering alone. The regularity and depth distribution of the red outer layer are consistent with a thermal gradient being applied to an originally homogeneous material and are incompatible with whole-rock, long-term geological heating, which would tend to alter the whole rock. From a technological point of view, this also demonstrates that these red vases were heated after manufacture. Additionally, some red vases contain macroscopic white inclusions that closely resemble those in some blue vases (Figs. 3 and 4). This supports the interpretation that at least some blue artefacts acquired a red hue.

Moreover, regarding the possible occurrence of naturally red serpentinite in Crete, the authors found no such rock during their surveys. Although Becker (1976) notes colour variations in serpentinite outcrops

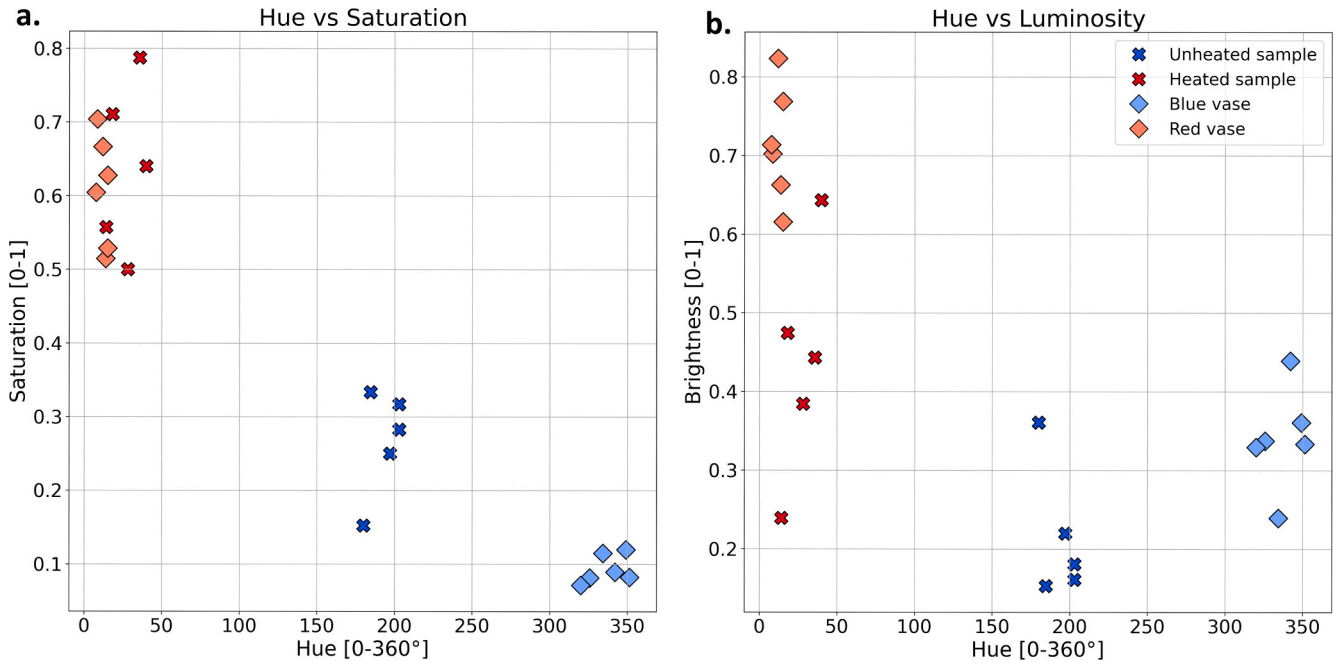

Fig. 10. a. Saturation, b. Luminosity versus Hue binary diagrams for hex colour sampled from experimental samples heated at 800 °C, and archaeological objects. Methodology can be found in Appendix A.6 Colour methodology. Colour sampling locations on archaeological objects are indicated by a circle in Figs. 3 and 4. Measurements of experimental samples were taken from the rock matrix. MS29 has been excluded from this graph due to an important red chromatic heterogeneity, rendering any single matrix sampling unrepresentative.

at Gonies, ranging from dark red to light green, the authors noticed on the field that the reddening is restricted to a superficial rind a few millimetres thick that does not penetrate the interior of the rock. This contrast in penetration depth (a superficial natural rind versus deeper gradients through the section of the vases) shows that the red colour noted by Becker cannot be the source of the vases. This also means that, up to this date at least, no naturally red serpentinite outcrop has ever been found on Crete.

4.2. *From blue to red: heating conditions*

To assess whether or not the red coloration of the vases was intentional, we first documented the materials and heating conditions required to produce it. Macroscopic analysis suggests that the red vases come from the serpentinite used for the blue vases at *Quartier Mu* (Figs. 3 and 4), a conclusion further supported by geochemical results showing an almost exact match between the two types (Fig. 6). This geochemical correspondence also rules out the use of additives with specific elements detectable by the pXRF, such as realgar (As_4S_4), cinnabar (HgS) or an addition of iron oxides (Fovakis et al., 2021).

However, the red vases exhibit significantly lower magnetic susceptibility values than the blue ones (Fig. 7). While an increase in magnetic susceptibility is usually interpreted as evidence of heating in chert (Borradaile et al., 1993; Larrasoaña et al., 2016) and other lithic clasts (Carrancho et al., 2014), a decrease in magnetic susceptibility has been linked to heating processes for some burnt clay, where high temperatures transform magnetite into weakly magnetic hematite (*e.g.*, Jordanova et al., 2019). Given that serpentinite naturally contains abundant magnetite, we suggest that a similar phase transformation occurred in the red vases. This interpretation is further supported by our heating experiments (Fig. 8, Figs. 11 and 12), which revealed a consistent decrease in magnetic susceptibility in the heated samples.

Our experiments on common Cretan serpentinite samples also indicate that a high temperature of at least 700 °C is required to produce a red coloration. This colour is certainly due in part to the formation of hematite inclusions (Fig. 11b, spectra 1–2), along with oxidised iron-rich phases, visible as microscopic to nanoscopic inclusions found within the olivine lattice dislocations (Knafelc et al., 2019; Kohlstedt et al., 1976), as can be seen in our μ-Raman spectra of olivine in heated MS43B (Fig. 11b, spectra 3–6). Our experiments also show that heat has a direct impact on the friability of the rock (especially evident when handling the samples), related to the volume decrease expected during rock de-serpentinisation (Klein and Le Roux, 2020). This is coherent with a visual comparison between the much better conservation state of blue vases compared to red vases. These experiments finally confirm that an atmospheric oxidising condition is enough to achieve the transformation, even if we cannot exclude the use of more specific heating processes (see Discussion 4.4).

4.3. *Intentional versus accidental heating*

The primary question surrounding the red vases found at *Quartier Mu* is whether their coloration was the result of deliberate artisanal production, involving voluntary and controlled heating, or merely a consequence of the accidental fire that destroyed the quarter. While the distinction between intentionally and accidentally heated objects is almost impossible to assess with certainty (Domanski and Webb, 2007, p. 159), the result of our experiments combined with contextual analyses strongly support Detournay's original interpretation that this red coloration of the vases was deliberately created through an artisanal production involving heating (Detournay, 1980).

Contextual analysis of Sector V indicates that only 7 out of the 101 objects found in this area have been described as "burnt" by the excavators (Dubois, 2017, and references therein). Given that red serpentinite needs to be heated to above 700 °C (see Discussion 4.2), an accidental destruction heating would imply that the destruction fire had to reach such temperatures. However, such accidental high temperatures require a process known as "flashover", where a fully-developed stage fire involves the simultaneous burning of all combustibles present in the room (Cunningham, 2007, p. 37; Kreimerman et al., 2022, p. 12). It is unlikely that a conflagration would have selectively heated only the red vases, while leaving unaffected the other categories of objects, of

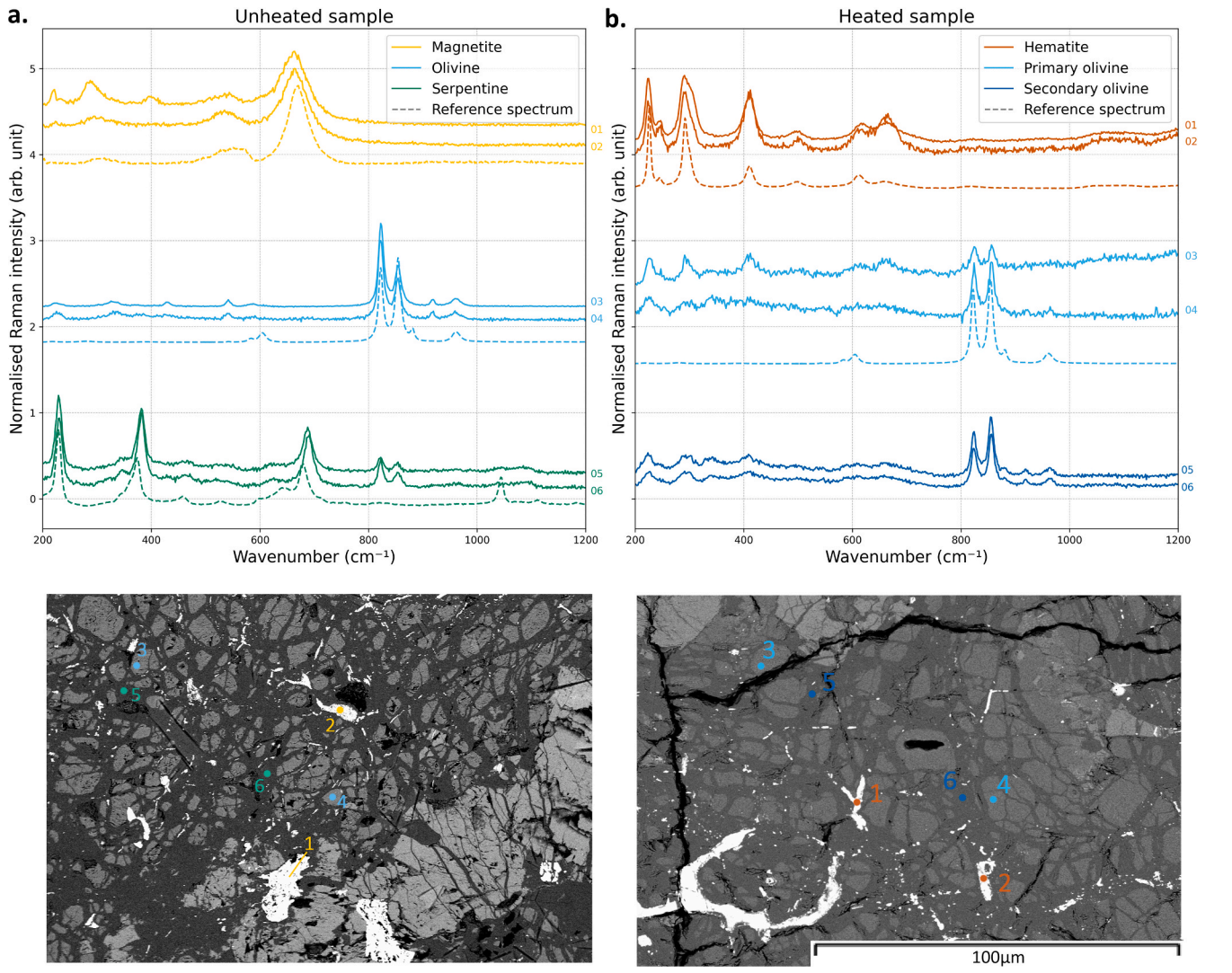

Fig. 11. Micro-Raman spectra collected at different points (1 to 6 on backscattered electron images above spectra plots) of a. unheated and b. heated MS43B. In b., secondary olivine designates the phase formed through serpentine transformation during heating (darker grey), while primary olivine refers to what was already olivine before heating (lighter grey). Reference spectra come from the open database REAP (Montagnac, 2019). Raman intensity has been normalised by a background correction with a polynomial baseline subtraction.

which only 7 out of 101 from Sector V of Building B show traces of burning. Therefore, we argue that the absence of evidence of widespread fire damage in this part of the building indicates that the red vases were not passively altered by the site's destruction but instead underwent a separate transformation process. This interpretation is supported by both experimental and contextual evidence, though future investigations into the thermal dynamics of the destruction event could provide further clarification.

Although the firing temperatures in kilns or firing artisanal structures during the Protopalatial period were less controlled than those in our experiments, Thér (2014) demonstrates that bonfires and pit firings, which are common methods for heating ceramics during this time (Caloi, 2019), could easily reach temperatures between approximately 600 °C and 1100 °C, with a median of around 750 °C (Thér, 2014). These values align closely with the range of temperatures obtained through our experimental heating results.

Lastly, contextual observations indicate that the red vases were found predominantly in specific areas alongside high-quality objects. Sector V of Building B, which is the place where most red vases were found (Fig. 2), yielded significant finds, including two copper daggers, 16 pieces of jewellery, 17 terracotta figurines, and 12 Chamaizi pots, which are often associated with ritual activities (Poursat, 2009). Room 5 of Sector V has even been compared to the Temple Repository of Knossos, a renowned sanctuary treasure (Poursat, 2009). While such an identification would require further substantiation, the association of red vases with some of the most valuable materials found at *Quartier Mu* suggests that these red vases hold a special status for the inhabitants.

4.4. Red hue conditions

The red vases exhibit variations in hue, both among themselves and compared to our experimental samples (Fig. 10). Factors such as heating rate or duration may account for some of the visual differences (Wadley et al., 2017, p. 375). However, our experiment focussed on replicating the mineralogical transformations identified through pMS analyses, especially those related to temperature and, to some extent, to raw material variations.

Our heating tests used material with similar geochemistry and mineralogy. However, colour differences still emerged depending on the starting material (Figs. 9 and 10). As the Bronze Age inhabitants of Crete likely supplied themselves in secondary sources such as rivers that offer well-sized cobbles ready to be used (Becker, 1975), the different hues seen in the red vases may reflect a difference in the protolith. Concerning the lighter red hue observed on the vases compared to our experimental

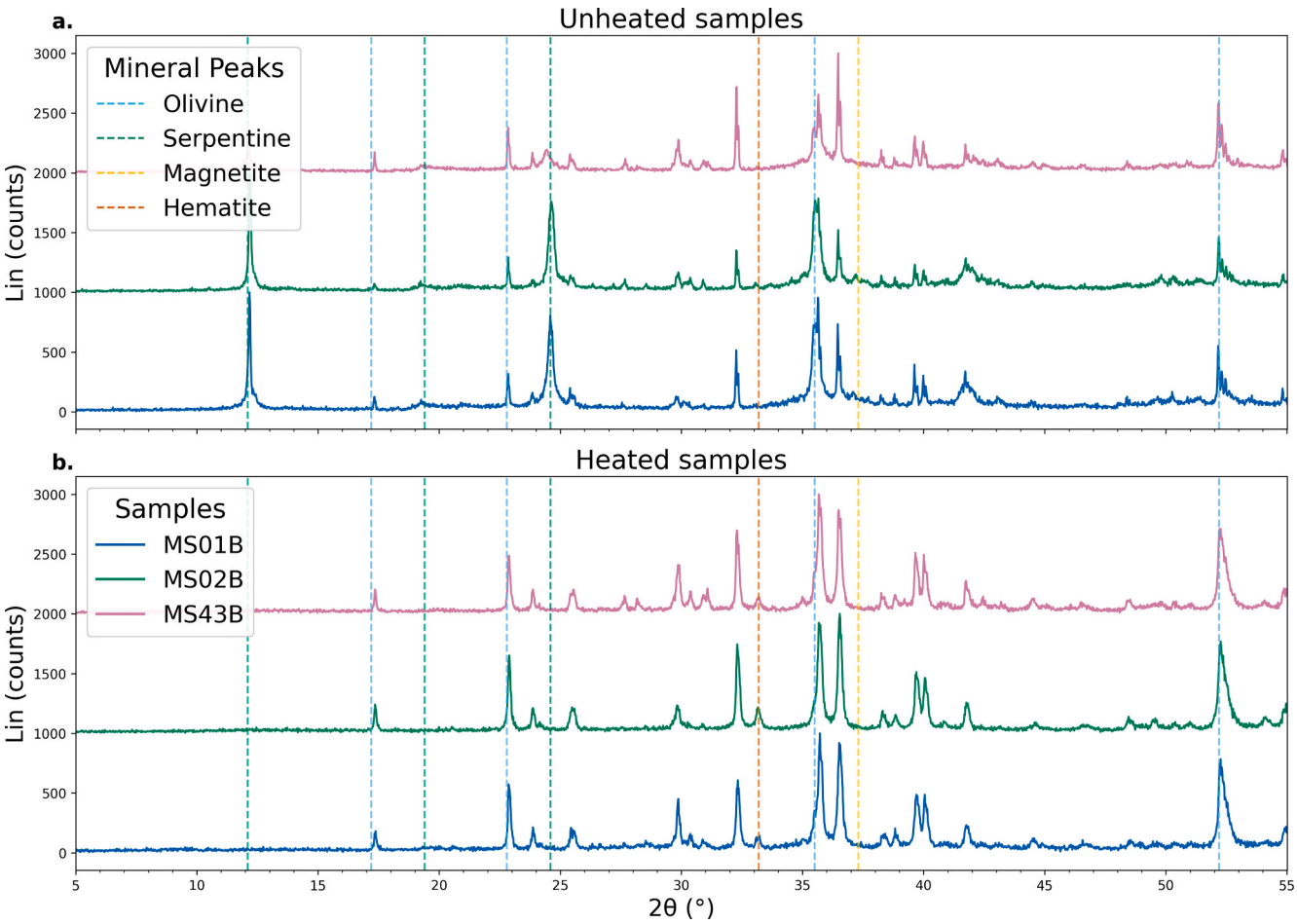

Fig. 12. XRD spectra of three samples a. before and b. after heating at 800 °C. Only selected peaks facilitating the comparison are highlighted here.

samples, unpublished analyses have suggested that Minoan serpentinite vases were composed of a lot of talc and chlorite (Rapp, 2009, p. 123)[3]. We propose that these minerals may have contributed to the lighter coloration by diluting the concentration of iron oxides responsible for the red hue. As talc is a light-coloured mineral with a low refractive index, its presence could reduce the intensity of the red hue by mixing with or covering the iron oxides, creating a more muted or pastel-like tone. Additionally, talc's high heat resistance and softness might influence the surface texture and light reflection during firing, further affecting the perceived colour, as has been highlighted by studies of talc-rich cooking stone vessels across periods and regions (Birney, 2008; Harrell and Brown, 2008; Truncer, 2004, p. 74). Heating experiments with protoliths that are closer to the archaeological material is a key direction to document this hypothesis. However, this will have to wait until the talc/chlorite content of the archaeological material is better documented.

4.5. *Unveiling new evidence of multicraft production and technological innovation in Quartier Mu?*

This case study of heated stone vessels is particularly significant, as deliberate heat treatment of stone to alter its appearance is almost unknown in Minoan archaeology. Beyond *Quartier Mu*, the only other evidence of red serpentinite comes from Myrtos-Pyrgos (Morero, 2014b) and from a few seals (Krzyszkowska, 2018). Considering the first one, given the well-documented connections between *Quartier Mu* and Myrtos-Pyrgos (Knappett, 1999), the Myrtos fragments are more plausibly interpreted as products of exchange or imitation rather than evidence of an independent local craft tradition.

The presence of red serpentinite among Cretan sealstones may be taken as evidence that naturally red serpentinite exists somewhere in Crete (Krzyszkowska, 2018). However, our experiments show that these red seals may similarly have been made from originally dark, naturally blueish serpentinite that was subsequently heated, whether accidentally or not. Such seal heating is not without precedent since some Middle Minoan IA (c. 2160/2025–1900 BCE) steatite seals and scarabs from the Mesara are known to have been fired to around 850 °C to become white and harder, possibly to imitate ivory (Pini, 1990, 2000; Sbonias, 1995, pp. 113–118).

One possible explanation for the technological experimentation with heated vases at *Quartier Mu* lies in the diverse craft activities taking place there, including both ceramic and stone-vase production. Since serpentinite can be heated under similar conditions to ceramic firing (see Discussion 4.3), this argument could be extended to suggest a form of co-production, where artisans from different crafts collaborated, or a multicraft production system, in which a single individual possessed expertise in multiple crafts (Shimada, 2007). The artisan of the *Atelier de Potier* is a good candidate for such multicraft practice, as the workshop presents work on ceramic vases and *appliqué* reliefs, both requiring a good handling of heating technology, as well as indirect evidence of stone-vase production, with two stone blanks and five drill cores (Poursat, 1996, p. 63; Morero, 2014b, p. 67). These brief considerations

[3] Additionally, as shown in Fig. 5, the magnesium content of the stone vases from *Quartier Mu* falls within the lower mid-range of worldwide serpentinites, which is coherent with previous observations on talc-rich serpentinite (Deschamps et al., 2013; Raia et al., 2022).

seek to contribute to the ongoing debate regarding potential interactions between ceramic- and stone-vase production during the Protopalatial period (Morero, 2014b; Palio, 2008, p. 285). A more targeted approach to the issue of multicraft production in *Quartier Mu* could potentially expand the evidence for technical exchanges between artisans beyond the limited data suggested in this study.

In summary, we propose that the red-heated serpentine vases from *Quartier Mu* may represent a limited experiment, born from the proximity of fire-related skills and stone-vase production. The reason this technology was not further used in Crete may lie in the significantly increased friability of the rock once heated, as observed in our experiments and in the red vases during handling. Heating appears to weaken the mineralogical structure, making the material more prone to breakage and potentially limiting the feasibility of producing or using such vessels on a larger scale.

The apparent uniqueness of heated stone vases within the Minoan world underscores the broader rarity of intentional visual stone heat treatment in the archaeological record. In their comprehensive review of heat treatment research in archaeology, Domanski and Webb (2007) only identified a few instances worldwide where heat was deliberately applied to ground stone artifacts to alter their appearance, with beads manufacture being the only examples. To our knowledge, the red-heated serpentinite vases from Malia stand out as the first known example of this practice applied to cobble-sized ground stone objects, making them a significant technological and cultural innovation.

5. Conclusion

The integration of non-invasive techniques, such as portable X-ray fluorescence (pXRF) and magnetic susceptibility (pMS), to experimental petrology provides a replicable framework for investigating the heat treatment of archaeological ground stone materials, without damaging the artifacts. So far, the red-heated serpentinite vases from *Quartier Mu* offer a unique and compelling example of intentional heat treatment applied to cobble-sized ground stone objects for aesthetic enhancement. These vases highlight the many technological experiments of Protopalatial artisans and contribute to our broader understanding of Minoan craft specialisation and multicraft practices.

CRediT authorship contribution statement

Killian Regnier: Writing – review & editing, Writing – original draft, Methodology, Investigation, Formal analysis, Conceptualization. **Antoine Triantafyllou:** Writing – review & editing, Methodology, Investigation. **Jean-Philippe Perrillat:** Writing – review & editing, Methodology, Formal analysis. **Charlotte Langohr:** Writing – review & editing. **Gilles Montagnac:** Writing – review & editing, Investigation. **Clémentine Fellah:** Writing – review & editing, Investigation. **Jérôme Bascou:** Writing – review & editing, Resources. **Anne-Christine Da Silva:** Writing – review & editing, Resources.

Declaration of competing interest

The authors declare that they have no known competing financial interests or personal relationships that could have appeared to influence the work reported in this paper.

Acknowledgments

The study of the archaeological objects was kindly granted by the Ephorate of Antiquities of Heraklion under permit number 423190 (11-09-2023), while the geological sampling was granted by the Hellenic Survey of Geology & Mineral Exploration under permits number 6953 (26-09-2023) and 1716 (05-04-2024). We would like to address our special acknowledgements to Angeliki Psaroudaki and Alexandros Sapountzakis for their assistance during the study of the archaeological materials, and to Ioannis Michalakis who facilitated the transfer of geological samples. We are also deeply thankful to Jean-Claude Poursat and the *École française d'Athènes* for granting permission to study this assemblage and for facilitating the administrative process. Killian Regnier is also particularly grateful to Nicolas Delmelle for his guidance in the grinding of samples used for XRD analyses, to Bastien Rueff for providing the background plan of *Quartier Mu* shown in Fig. 2, and to Roxane Dubois for sharing her unpublished master's thesis database on *Quartier Mu*. The authors thank the two anonymous reviewers for their careful reading and constructive comments, and Hilary Tresidder for English proofreading.

Funding

K. R. was supported by a *Fonds de la Recherche Scientifique* (FNRS) funded PhD studentship (grant numbers 40011988 and 4002374). The on-field research also benefitted from mobility grants awarded by the FNRS (grant number 40019514). A.T. acknowledges support from the *Université Claude Bernard de Lyon* with the "*BQR – EC 2022*" as well as for the *"AAP LYON 1 – Équipement de Recherche 2022"* granted to the LGL-TPE and the FAIRE platform (https://lgltpe.fr/tous-plateforme/fair/). The Raman facility REAP (Raman Experiment for Astrobiology and Planetology) in Lyon (France) is supported by the *Institut National des Sciences de l'Univers* (INSU). It is a contribution of the LabEx Lyon Institute of Origins (ANR-10-LABX-0066), within the "*Investissements d'Avenir*" programme (ANR-11-IDEX-0007) at the *Université de Lyon*.

Appendix A. Methodological details

Appendix A.1 Portable X-Ray Fluorescence (pXRF) analyses

The SciAPS X-505 pXRF is equipped with a 200 μA Rh anode X-Ray tube and a 20 mm^2 silicon drift detector with a resolution of 140 eV at Mn kalpha (manufacturer's manual, https://www.sciaps.com/products/xrf/x-505). All analyses were undertaken under the constructor *mining* (10 and 40 keV) calibration, with 30 s per voltage. This duration was selected after tests on six serpentinite pressed pellet samples that showed an average relative difference of <0.5 % for Mg, Al, Si, K, Ca, P, Mn, and Fe between 30 and 60 s of analyses per voltage. Analytical precision was validated through these tests (data available upon request). A 4 μm polypropylene window was used; no vacuum or helium flush was used. Accuracy tests on 27 magmatic reference samples, including mafic rocks, showed an accuracy above 95 % – except for Al, which reached 90 % – for all these elements after a simple linear corrective offset adapted to each element was made following the methodology of (Da Silva et al., 2023). The preparation and laboratory analyses of these reference samples are described in (Govindaraju, 1994). Mg, Al, Si, K, Ca, P, Mn, and Fe were converted to their corresponding oxides. A homemade serpentinite calibration is currently underway.

As suggested by (Adams et al., 2021) in their non-invasive workflow for mafic and ultramafic rocks, pXRF analyses should be filtered based on their total major concentrations to ensure that data are not too corrupted. Because serpentinite can contain up to 15 wt% of water, which is undetected by pXRF, a range of sum oxides from 80 % to 120 % has been used for filtering. Between 1 and 10 analyses have been processed per object, depending on several factors such as the state of preservation, the adding of a glue during the conservation process or the possibility of analysing a flat surface. Geochemical data can be found in Appendix B. Supplementary data.

Appendix A.2 Portable magnetic susceptibility (pMS) methodology

The Bartington MS2K scanner generates a weak alternating magnetic field that interacts with the material's internal magnetic properties, thus creating a magnetic response measured by the MS3 sensor. Measurements are recorded in dimensionless SI units, under a resolution of 2 μSI

(Deng, 2015). The MS2K has a response depth of 50 % at 3 mm and 10 % at 8 mm (manufacturer's manual, https://www.geostudiastier.it/writable/public/file/brochure_it_105.pdf). Therefore, analysis surfaces were selected only on areas where the vase thickness exceeded 1 cm in order to eliminate the need for thickness correction (Williams-Thorpe et al., 2007). Following the methodology of (Triantafyllou et al., 2021), each sample was analysed ten times consecutively, with each analysis lasting 10 s. These measurements were flanked by two 10-second blank analyses for instrument drift correction. At the beginning and end of each day, the reference material from the constructor was analysed and showed an average offset of 1.2 % from the manufacturer reference value. At least ten analyses were made per archaeological object and geological sample. pMS data can be found in Appendix B. Supplementary data.

Appendix A.3 X-ray diffraction (XRD) methodology

X-ray powder diffraction measurements were carried out on three samples: MS01B, MS02B and MS43B, on both unheated and heated materials, after the samples were ground to a 2–3 μm grain size in diameter. Spectra were acquired at the "*Centre de Diffractométrie Henri Longchambon*" University of Lyon 1, on a Bragg-Brentano Bruker D8 Advance diffractometer working with Cu anticathode (40 kV, 40 mA) at a monochromatic radiation $\lambda = 1.54056$ Å. The data were collected over an angular range of $2\theta = 5°$-$90°$ with a 0.006° step, and 10 s step time. The 2θ diffraction patterns were processed using the GSAS package (Larson and Von Dreele, 1994) to retrieve the product phases, their unit-cell parameters and their proportions. XRD raw data can be found in Appendix B. Supplementary data.

Appendix A.4 Micro-Raman scattering methodology

μ-RS is a non-invasive analytical technique that uses Raman scattering to identify molecular and crystal structures based on their vibrational modes. One sample, MS43B, was spatially characterised by μ-RS at the Raman facility REAP in Lyon (France). μ-Raman spectra were collected using a confocal LabRam HR800 spectrometer characterised by a local length of 800 mm and equipped with a 532 nm laser and a 600-grooves-per-millimetre grating (resolution <4 cm^{-1}). A 100 × long working distance microscope objective condensed the laser beam on to the sample and collected the backscattered Raman signal. A low laser power (<1 eV) was employed to prevent converting Fe(II)-containing minerals to Fe(III)-oxides (Colomban, 2011; de Faria et al., 1997). The integration time varied based on the analysis point and the degree of fluorescence observed. μ-RS raw data can be found in Appendix B. Supplementary data.

Appendix A.5 Scanning electron microscopy – energy-dispersive spectroscopy (SEM-EDS) methodology

Scanning electron microscopy was used to study the structural organisation and chemical phase distribution of experimental samples. The JEOL IT800HL SEM at the ENS Lyon microscopy platform is equipped with several imaging detectors and an EDX detector (X-Max 50, Oxford Instruments) for elemental spot analysis. Samples were observed with a backscattered electron detector and analysed with the EDX detector at 15 kV, with a probe current of 10nA and a working distance of 9 mm.

Appendix A.6 Colour comparison methodology

Photographs were taken with a Canon M50 Mark II, equipped with an EF-M 15–45 mm lens, and put on a static tripod. Manual options were set up with a focal distance of 28 mm, an aperture of f/13, an obturation time of 1/50 and ISO 500. Subjects were placed in a lightbox to ensure optimal lightning conditions. Image colours were calibrated with a Calibrite ColorChecker Classic. The HSV (Hue, Saturation, Value) colour was obtained using the Photoshop eyedropper tool with a sampling size of 31x31 pixels. Previous studies comparing eyedropper sampling of calibrated images with spectrophotometer results have shown that this leads to similar results between both methods (*e.g.*, Dardenay, Mulliez and Mora, 2017). HSV separates chromatic content (hue and saturation) from brightness (value), making it easier to interpret colour variations related to heating or material differences in archaeological samples.

Appendix B. Supplementary data

The data and code that support the findings of this study are openly available on Zenodo at https://doi.org/10.5281/zenodo.17296603.

Data availability

The data and code that support the findings of this study are openly available on Zenodo at https://doi.org/10.5281/zenodo.17296603.

Bibliography

Adams, C., Dentith, M., Fiorentini, M., 2021. Characterization of altered mafic and ultramafic rocks using portable XRF geochemistry and portable Vis-NIR spectrometry. Geochem. Explor. Environ. Anal. 21, geochem2020-065. https://doi.org/10.1144/geochem2020-065.

Becker, M., 1975. Minoan sources for steatite and other stones used for vases and artifacts: a preliminary report. Αρχαιολογικόν Δελτίον 30A, 242–252.

Becker, M., 1976. Soft-stone sources on crete. J. Field Archaeol. 3, 361–374. https://doi.org/10.1179/009346976791490457.

Bevan, A., 2007. Stone Vessels and Values in the Bronze Age Mediterranean. Cambridge.

Birney, K., 2008. Tracking the cooking pot à la stéatite: signs of cyprus in iron age Syria. Am. J. Archaeol. 112, 565–580. https://doi.org/10.3764/aja.112.4.565.

Bloise, A., Catalano, M., Barrese, E., Gualtieri, A.F., Bursi Gandolfi, N., Capella, S., Belluso, E., 2016. TG/DSC study of the thermal behaviour of hazardous mineral fibres. J. Therm. Anal. Calorim. 123, 2225–2239. https://doi.org/10.1007/s10973-015-4939-8.

Bloise, A., Miriello, D., 2018. Multi-analytical approach for identifying asbestos minerals in situ. Geosciences 8, 133. https://doi.org/10.3390/geosciences8040133.

Bonnemains, D., Carlut, J., Escartín, J., Mével, C., Andreani, M., Debret, B., 2016. Magnetic signatures of serpentinization at ophiolite complexes. Geochem. Geophys. Geosyst. 17, 2969–2986. https://doi.org/10.1002/2016GC006321.

Borradaile, G.J., Jackson, M., 2004. Anisotropy of magnetic susceptibility (AMS): magnetic petrofabrics of deformed rocks. Geol. Soc., Lond. Special Publ. 238, 299–360. https://doi.org/10.1144/GSL.SP.2004.238.01.18.

Borradaile, G.J., Kissin, S.A., Stewart, J.D., Ross, W.A., Werner, T., 1993. Magnetic and optical methods for detecting the heat treatment of chert. J. Archaeol. Sci. 20, 57–66. https://doi.org/10.1006/jasc.1993.1004.

Caloi, I., 2019. Breaking with tradition? The adoption of the wheel-throwing technique at Protopalatial Phaistos: combining macroscopic analysis, experimental archaeology and contextual information. Annu. Sc. Archeol. Atene Mission. Ital. Oriente 97, 9–25.

Carrancho, Á., Morales, J., Goguitchaichvili, A., Alonso, R., Terradillos, M., 2014. Thermomagnetic monitoring of lithic clasts burned under controlled temperature and field conditions. Implications for archaeomagnetism. Geofís. Int. 53, 473–490. https://doi.org/10.1016/S0016-7169(14)70079-0.

Chen, H., Tao, C., Revil, A., Zhu, Z., Zhou, J., Wu, T., Deng, X., 2021. Induced polarization and magnetic responses of serpentinized ultramafic rocks from mid-ocean ridges. J. Geophys. Res. Solid Earth 126. https://doi.org/10.1029/2021JB022915.

Colomban, P., 2011. Potential and Drawbacks of Raman (Micro)spectrometry for the Understanding of Iron and Steel Corrosion, in: Chiaberge, M. (Ed.), New Trends and Developments in Automotive System Engineering. Turin, pp. 567-584. Doi: 10.5772/13436.

Cunningham, T., 2007. Havoc: the destruction of power and the power of destruction in Minoan Crete, in: Driessen J., Bretschneider J., van Lerberghe K. (Eds.), Power and Architecture: Monumental Public Architecture in the Bronze Age Near East and Aegean. Leuven, pp. 23–43.

Da Silva, A.C., Triantafyllou, A., Delmelle, N., 2023. Portable x-ray fluorescence calibrations: workflow and guidelines for optimizing the analysis of geological samples. Chem. Geol. 623, 121395. https://doi.org/10.1016/j.chemgeo.2023.121395.

Dardenay, A., Mulliez, M., Mora, P., 2017. Reconstruction of ancient wall paintings: digital painting and three-dimensional restoration of the House of Neptune and Amphitrite in Herculaneum, in: Mulliez, M. (Ed.), Virtual Retrospect, Restituer Les Couleurs / Reconstruction of Polychromy. Ausonius, Pessac, France, pp. 67–77.

de Faria, D.L.A., Venâncio Silva, S., de Oliveira, M.T., 1997. Raman microspectroscopy of some iron oxides and oxyhydroxides. J. Raman Spectrosc. 28, 873–878. https://doi.org/10.1002/(SICI)1097-4555(199711)28:11<873::AID-JRS177>3.0.CO;2-B.

Debret, B., 2013. Serpentinites, vecteurs des circulations fluides et des transferts chimiques de l'océanisation à la subduction: exemple dans les Alpes occidentales

(Unpublished PhD thesis). Université Blaise Pascal Clermont Auvergne, Clermont-Ferrand.
Deng, D.N., 2015. A comparative study of hand-held magnetic susceptibility instruments. Laurentian University of Sudbury, Sudbury. Unpublished master's thesis.
Deschamps, F., Godard, M., Guillot, S., Hattori, K., 2013. Geochemistry of subduction zone serpentinites: a review. Lithos 178, 96–127. https://doi.org/10.1016/j.lithos.2013.05.019.
Detournay, B., 1980. Vases de pierre, in: Poursat, J.-C., Detournay, B., Vandeabeele, F. (Eds.), Fouilles Exécutées à Mallia : Le *Quartier Mu*. II, Vases de Pierre et de Métal, Vannerie, Figurines et Reliefs d'applique, Éléments de Parure et de Décoration, Armes, Sceaux et Empreintes, Études Crétoises. Athens, pp. 19–69.
Dlugogorski, B.Z., Balucan, R.D., 2014. Dehydroxylation of serpentine minerals: implications for mineral carbonation. Renew. Sustain. Energy Rev. 31, 353–367. https://doi.org/10.1016/j.rser.2013.11.002.
Domanski, M., Webb, J., 2007. A review of heat treatment research. Lithic Technol. 32, 153–194. https://doi.org/10.1080/01977261.2007.11721052.
Driessen, J., 2024. Regionalism and/or standardisation? A non-ceramic view on Protopalatial Crete., in: Caloi, I., Doudalis, G. (Eds.), Protopalatial Pottery. Relative Chronology and Regional Differences in Middle Bronze Age Crete. Louvain-la-Neuve, pp. 1–24.
Dubois, R., 2017. Le *Quartier Mu* (Malia, Crète) : étude fonctionnelle d'un important complexe archéologique du Minoen Moyen IIB (Unpublished master's thesis. Université catholique de Louvain-la-Neuve, Louvain-la-Neuve.
Flouda, G., Philippidis, A., Mikallou, A., Anglos, D., 2020. Materials analyses of stone artifacts from the EBA to MBA Minoan Tholos tomb P at Porti, Greece (Crete), by means of Raman spectroscopy: results and a critical assessment of the method. J. Archaeol. Sci. Rep. 32, 102436. https://doi.org/10.1016/j.jasrep.2020.102436.
Forster, N., Grave, P., Vickery, N., Kealhofer, L., 2011. Non-destructive analysis using PXRF: methodology and application to archaeological ceramics. X-Ray Spectrom. 40, 389–398. https://doi.org/10.1002/xrs.1360.
Fovakis, P.E., Ganetsos, T., Daskalakis, N.G., 2021. Study and analyses of pigments in minoan larnakes from the peripheral unit of rethymnon (Crete) applying non-destructive techniques: preliminary results. Archaeology 9, 94–100.
Frerebeau, N., Pernot, M., 2018. Dans la chaleur des fours : que restituer des pratiques des céramistes des sociétés anciennes? ArcheoSciences. Rev. Archéom. 95–105. https://doi.org/10.4000/archeosciences.6007.
Govindaraju, K., 1994. Compilation of working values and sample description for 383 geostandards. Geostand. Newsl. 18, 1–158. https://doi.org/10.1046/j.1365-2494.1998.53202081.x-i1.
Graham, J.W., 1953. Changes of ferromagnetic minerals and their bearing on magnetic properties of rocks. J. Geophys. Res. 58, 243–260. https://doi.org/10.1029/JZ058i002p00243.
Grave, P., Attenbrow, V., Sutherland, F., Pogson, R., Forster, N., 2012. Non-destructive pXRF of Mafic stone tools. J. Archaeol. Sci. 39, 1674–1686. https://doi.org/10.1016/j.jas.2011.11.011.
Harrell, J.A., Brown, V.M., 2008. Discovery of a medieval Islamic Industry for Steatite Cooking Vessels in Egypt's Eastern Desert. In: Rowan, Y.M., Ebeling, J.R. (Eds.), New Approaches to Old Stones. Routledge, London, pp. 41–65.
Hodel, F., Macouin, M., Triantafyllou, A., Carlut, J., Berger, J., Rousse, S., Ennih, N., Trindade, R.I.F., 2017. Unusual massive magnetite veins and highly altered Cr-spinels as relics of a Cl-rich acidic hydrothermal event in Neoproterozoic serpentinites (Bou Azzer ophiolite, Anti-Atlas, Morocco). Precambr. Res. 300, 151–167. https://doi.org/10.1016/j.precamres.2017.08.005.
Jordanova, N., Jordanova, D., Barrón, V., Lesigyarski, D., Kostadinova-Avramova, M., 2019. Rock-magnetic and color characteristics of archaeological samples from burnt clay from destructions and ceramics in relation to their firing temperature. Archaeol. Anthropol. Sci. 11, 3595–3612. https://doi.org/10.1007/s12520-019-00782-y.
Klein, F., Le Roux, V., 2020. Quantifying the volume increase and chemical exchange during serpentinization. Geology 48, 552–556. https://doi.org/10.1130/G47289.1.
Knafelc, J., Filiberto, J., Ferré, E.C., Conder, J.A., Costello, L., Crandall, J.R., Dyar, M.D., Friedman, S.A., Hummer, D.R., Schwenzer, S.P., 2019. The effect of oxidation on the mineralogy and magnetic properties of olivine. Am. Mineral. 104, 694–702. https://doi.org/10.2138/am-2019-6829.
Knappett, C., 1999. Assessing a Polity in Protopalatial Crete: The Malia-Lasithi State. Am. J. Archaeol. 103, 615–639. https://doi.org/10.2307/507075.
Kohlstedt, D.L., Goetze, C., Durham, W.B., Vander Sande, J., 1976. New technique for decorating dislocations in olivine. Science 191, 1045–1046. https://doi.org/10.1126/science.191.4231.1045.
Kreimerman, I., Garfinkel, Y., Hasel, M.G., Shahack-Gross, R., 2022. High-resolution investigation of a conflagration event in the north-east temple at Lachish via integration of forensic, stratigraphic and geoarchaeological evidence: a model for studying architectural destruction by fire. J. Archaeol. Sci. Rep. 46, 103705. https://doi.org/10.1016/j.jasrep.2022.103705.
Krzyszkowska, O., 2018. Materials, motifs and mobility in Minoan glyptic, in: Πεπραγμένα ΙΒ΄ Διεθνούς Κρητολογικού Συνεδρίου. Proceedings of the 12th International Cretological Congress of Cretan Studies. 21-25 October 2016. Heraklion, pp. 1–17.
Lagoeiro, L.E., 1998. Transformation of magnetite to hematite and its influence on the dissolution of iron oxide minerals. J. Metam. Geol. 16, 415–423. https://doi.org/10.1111/j.1525-1314.1998.00144.x.
Larrasoaña, J.C., Beamud, E., Olivares, M., Murelaga, X., Tarriño, A., Baceta, J.I., Etxebarria, N., 2016. Magnetic properties of cherts from the basque-cantabrian basin and surrounding regions: archeological implications. Front. Earth Sci. 4. https://doi.org/10.3389/feart.2016.00035.
Larson, C., Von Dreele, B., 1994. General structure analysis system. Los Alamos Natl. Lab. 86, 748–786.
Martha, S.O., Dörr, W., Gerdes, A., Krahl, J., Linckens, J., Zulauf, G., 2017. The tectonometamorphic and magmatic evolution of the Uppermost Unit in central Crete (Melambes area): constraints on a late cretaceous magmatic arc in the Internal Hellenides (Greece). Gondw. Res. 48, 50–71. https://doi.org/10.1016/j.gr.2017.04.004.
Martha, S.O., Zulauf, G., Dörr, W., Binck, J.J., Nowara, P.M., Xypolias, P., 2019. The tectonometamorphic evolution of the uppermost unit south of the Dikti mountains. Crete. Geol. Mag. 156, 1003–1026. https://doi.org/10.1017/S0016756818000328.
McCammon, C., 2005. The paradox of mantle redox. Science 308, 807–808. https://doi.org/10.1126/science.1110532.
Menzel, M.D., Garrido, C.J., López Sánchez-Vizcaíno, V., Hidas, K., Marchesi, C., 2019. Subduction metamorphism of serpentinite-hosted carbonates beyond antigorite-serpentinite dehydration (Nevado-Filábride complex, Spain). J. Metam. Geol. 37 (5), 681–715. https://doi.org/10.1111/jmg.12481.
Montagnac, G., 2019. SSHADE/REAP: Raman Experiments for Astrobiology and Planetology. Doi: 10.26302/SSHADE/REAP.
Morero, E., 2016. Méthodes d'analyse des techniques lapidaires. Les vases de pierre en Crète à l'âge du Bronze (IIIe-IIe millénaire av. J.-C.). Paris.
Morero, E., 2014a. Les techniques de fabrication des vases de pierre, in: Poursat, J.-C. (Ed.), Fouilles Exécutées à Malia, Le *Quartier Mu* V, Vie Quotidienne et Techniques Au Minoen Moyen II, Études Crétoises 34. Athens, pp. 67–85.
Morero, E., 2014b. Les techniques de fabrication de la vaisselle de pierre de Myrtos-Pyrgos. Bull. De Corresp. Hell. 138, 329–360. https://doi.org/10.3406/bch.2014.8024.
Palio, O., 2008. I Vasi in Pietra Minoici da Festòs. Studi di Archeologia Cretese, Padoua.
Pini, I., 2000. Eleven Early Cretan Scarabs. In: Karetsou, A., Andreadaki-Vlazaki, M., Papadakis, N. (Eds.), Κρήτη – Αίγυπτος. Πολιτισμικοί Δεσμοί Τριών Χιλιετιών, Exhibition Catalogue, Heraklion, pp. 107–113.
Pini, I., 1990. Eine Frühkretische Siegelwerkstatt?, in: Kapsomenos, E., Andreadaki-Vlazaki , M., Andrianakis M., Papadopoulou E. (Eds.), Pepragmena Tou ST' Diethnous Kritologikou Synedriou, A2. Chania, pp. 115–127.
Poursat, J.-C., 2009. Cult activity at Malia in the Protopalatial Period. Hesperia Suppl. 42, 71–78.
Poursat, J.-C., 1996. Fouilles exécutées à Malia : le *Quartier Mu*. III, Les artisans minoens : les maisons-ateliers du *Quartier Mu*. Athens.
Poursat, J.-C., Knappett, C., 2005. Fouilles exécutées à Malia : le *Quartier Mu*. IV, La poterie du minoen moyen II : production et utilisation, Études crét. Athens.
Punturo, R., Cirrincione, R., Pappalardo, G., Mineo, S., Fazio, E., Bloise, A., 2018. Preliminary laboratory characterization of serpentinite rocks from Calabria (southern Italy) employed as stone material. J. Mediterranean Earth Sci. 10. https://doi.org/10.3304/JMES.2018.017.
Raia, N.H., Whitney, D.L., Teyssier, C., Lesimple, S., 2022. Serpentinites of different tectonic origin in an exhumed subduction complex (new Caledonia, SW Pacific). Geochem., Geophys., Geosyst. 23, e2022GC010395. https://doi.org/10.1029/2022GC010395.
Rapp, G., 2009. Archaeomineralogy. Heidelberg. Doi: 10.1007/978-3-540-78594-1.
Relaki, M., Tsoraki, C., 2015. Variability and differentiation. A first look at the patterns of use and deposition of stone vases in the Petras cemetery, in: Tsipopoulou, M. (Ed.), Petras, Siteia the Pre- and Proto-Palatial Cemetery in Context. Athens, pp. 159–178.
Rochette, P., Jackson, M., Aubourg, C., 1992. Rock magnetism and the interpretation of anisotropy of magnetic susceptibility. Rev. Geophys. 30, 209–226. https://doi.org/10.1029/92RG00733.
Sbonias, K., 1995. Frükretische Siegel: Ansätze für eine Interpretation der sozial-politischen Entwicklung auf Kreta während der Frühbronzezeit. Oxford.
Schmid, M., Treuil, R., 2017. Fouilles exécutées à Malia, le *Quartier Mu* VI. Architecture minoenne à Malia. Les bâtiments principaux du *Quartier Mu* (A, B, D, E) (Minoen Moyen II), Études crétoises, 36. Athens.
Schwertmann, U., 1993. Relations Between Iron Oxides, Soil Color, and Soil Formation, in: Bigham J. M., Ciolkosz E. J. (Eds.), Soil Color. Madison, pp. 51–69. Doi: 10.2136/sssaspecpub31.c4.
Shimada, I., 2007. Craft Production in Complex Societies: Multicraft and Producer Perspectives. Salt Lake City.
Thér, R., 2014. Identification of pottery firing structures using the thermal characteristics of firing. Archaeom 56, 78–99. https://doi.org/10.1111/arcm.12052.
Tortorici, L., Catalano, S., Cirrincione, R., Tortorici, G., 2012. The Cretan ophiolite-bearing mélange (Greece): a remnant of Alpine accretionary wedge. Tectonophys 568–569, 320–334. https://doi.org/10.1016/j.tecto.2011.08.022.
Triantafyllou, A., Mattielli, N., Clerbois, S., Da Silva, A.C., Kaskes, P., Claeys, P., Devleeschouwer, X., Brkojewitsch, G., 2021. Optimizing multiple non-invasive techniques (PXRF, pMS, IA) to characterize coarse-grained igneous rocks used as building stones. J. Archaeol. Sci. 129, 105376. https://doi.org/10.1016/j.jas.2021.105376.
Truncer, J., 2004. In: Steatite Vessel Manufacture in Eastern North America. University of Michigan Press, Ann Arbor, MI. https://doi.org/10.30861/9781841716718.
Wadley, L., de la Peña, P., Prinsloo, L.C., 2017. Responses of south African agate and chalcedony when heated experimentally, and the broader implications for heated archaeological minerals. J. Field Archaeol. 42, 364–377. https://doi.org/10.1080/00934690.2017.1337438.
Warren, P., 1969. Minoan Stone Vases. Cambridge.
Williams-Thorpe, O., Jones, M., Webb, P., Rigby, I., 2007. Magnetic susceptibility thickness corrections for small artefacts and comments on the effects of "Background" materials. Archaeom 42, 101–108. https://doi.org/10.1111/j.1475-4754.2000.tb00868.x.